

Ferroelectric properties and leakage current mechanisms in $\text{SrBi}_2(\text{V}_{0.1}\text{Nb}_{0.9})_2\text{O}_9$ (SBVN) thin films

S. Ezhilvalavan^{a,*}, Victor Samper^a, Toh Wei Seng^b, Xue Junmin^b, John Wang^b

^a Institute of Bioengineering and Nanotechnology, 51, Science Park Road #01-01/10, The Aries, Singapore Science Park II, Singapore 117586, Singapore

^b Department of Materials Science, National University of Singapore, 10 Kent Ridge Crescent, Singapore 119260, Singapore

Received 1 December 2003; received in revised form 10 December 2003; accepted 22 December 2003

Available online 6 May 2004

Abstract

Ferroelectric properties and leakage current mechanisms of polycrystalline $\text{SrBi}_2(\text{V}_{0.1}\text{Nb}_{0.9})_2\text{O}_9$ (SBVN) thin films were studied. SBVN films were deposited on $\text{Pt}/\text{SiO}_2/n\text{-Si}$ substrate by rf-magnetron sputtering and then annealed at 700°C for 60 min in air. The films showed excellent ferroelectric properties in terms of larger remnant polarization ($2P_r$) of $25\text{ }\mu\text{C}/\text{cm}^2$ ($2E_c \sim 200\text{ kV}/\text{cm}$), fatigue free characteristics up to $\geq 10^8$ switching cycles and low current density of $10^{-8}\text{ A}/\text{cm}^2$ at $100\text{ kV}/\text{cm}$. XRD and SEM investigations indicate that the sputtered films exhibit a dense, well crystallized microstructure having random orientations and with a rather smooth surface morphology. The improved ferroelectric and leakage current characteristics obtained at lower processing temperature are attributed to the larger polarizability attained through increased rattling space in the distorted $\text{Nb}(\text{V})\text{O}_6$ of the perovskite block due to the partial substitution of Nb with smaller V ions. The leakage current density of the SBVN thin films was studied at higher temperatures and the data were fitted with the Schottky and Poole–Frenkel emission models.

© 2004 Elsevier Ltd and Techna Group S.r.l. All rights reserved.

Keywords: A. Films; C. Electrical conductivity; C. Ferroelectric properties; D. Perovskites; E. Functional applications

1. Introduction

There has been renewed interest in bismuth layer oxide thin films because of their potential applications as non-volatile memory devices [1,2]. $\text{SrBi}_2\text{Nb}_2\text{O}_9$ (SBN) and $\text{SrBi}_2\text{Ta}_2\text{O}_9$ (SBT) have been the most intensively studied compounds among bismuth layer-structured ferroelectrics, due to their superior properties such as low leakage current density, low operating voltage, fast switching and fatigue endurance up to 10^{12} switching cycles [3–5].

Recently, we have reported the reduction of processing temperature of SBN by partial substitution of Nb^{5+} ion by V^{5+} ion [6,7]. Accordingly, SBN bulk ceramics crystallize at low temperature upon vanadium substitution and also show enhanced dielectric and ferroelectric properties. Wu and Cao [8] have also reported similar findings for V doped SBT ceramics. However, for SBT or SBN thin films, the influ-

ence of vanadium addition on the ferroelectric behavior is not satisfactorily worked out. Chen et al. [9] and Barz et al. [10] studied the effect of vanadium doping on the ferroelectric properties of SBT films fabricated by sol–gel process. The results obtained by Chen et al. showed improved performance of V-doped SBT films in terms of higher remnant polarization and better fatigue resistance which are contrary to the observations of Barz et al. for vanadium added SBT films. However, the observations of Das et al. [11] on the ferroelectric behavior of pulsed laser deposited V-doped SBT films are in line with Chen et al. Therefore, a detailed investigation is mandatory to envisage the influence of vanadium addition on the ferroelectric properties of SBN similar in composition and structure as that of SBT but processed by a well established fabrication method, namely rf-sputtering.

Although as-deposited SBN films have low leakage characteristics, high temperature treatments, which are necessary for their crystallization and integration into microelectronic circuits, resulted in drastic increase of leakage current. This obviously limits their use in NVFeRAMs in terms of refresh

* Corresponding author. Fax: +65-6874-9341.

E-mail address: valavan@ibn.a-star.edu.sg (S. Ezhilvalavan).

characteristics of the cell. Hence, it is important to study the various leakage mechanisms in the polycrystalline films in order to improve their ferroelectric and dielectric properties. Some reports exist in literature on the leakage current mechanisms in SBN thin films [12,13]. However, to the best of our knowledge, there has been no report on the ferroelectric behavior and the leakage current characteristics of vanadium doped SBN thin films fabricated by rf-sputtering. In this article, we report the effect of 10 at.% vanadium substitution at Nb-site and studied the growth behavior of random oriented SBVN ferroelectric thin films fabricated by rf-magnetron sputtering. We have examined the ferroelectric, dielectric and leakage current characteristics of sputtered SBVN films with definite conclusion and quality for the application in NVFeRAMs.

2. Experimental procedures

Bismuth layered ferroelectric thin films of composition $\text{SrBi}_2(\text{Nb}_{0.9}\text{V}_{0.1})_2\text{O}_9$ (SBVN) were grown on Pt/TiO₂/SiO₂/Si substrate using rf-magnetron sputtering from a high purity ceramic target of 2 in. diameter. The SBVN targets with 5 wt.% excess bismuth oxide were prepared by solid state reaction process and sintered at 900 °C for 2 h. All films were prepared at a fixed power of 75 W (power density $\sim 3.8 \text{ W/cm}^2$) and Ar pressure of 10 mTorr. The as-grown film was subjected to annealing at 700 °C for 1 h in air. The film thickness was determined by examining the cross-section of the film via scanning electron microscopy (SEM, XL30 FEG Philips). The blanket Pt underneath the SBVN film was used as the bottom electrode for electrical testing. Pt top electrodes with diameters of 150–350 μm were dc-sputtered through a shadow mask so as to define planar capacitor structure. The phase formation and crystallinity of the films were analyzed using X-ray diffraction (XRD, X'pert Philips). The dielectric measurements were carried out at frequencies 100 Hz to 1 MHz using Solartron impedance/gain-phase analyzer (SI 1260, England) with a signal voltage of 50 mV. The ferroelectric properties were measured with a precision workstation (Radiant Technologies). The I – V characteristics were evaluated using HP4145B Semiconductor parameter analyzer, and the measurement was carried out with a sufficient charging time to reach the steady state dc leakage regime.

3. Results and discussion

The XRD patterns of SBVN thin films post-annealed at 700 °C for 1 h is shown in Fig. 1. It was observed that the film was fully crystallized and exhibited random orientation. The diffraction lines (1 1 5), (0 2 0), (2 2 0) and (1 3 5) are more pronounced than (0 0 8) and (0 0 1 0) lines, which indicates that the preferred orientation along (0 0 1) direction is suppressed and the annealed film may show predom-

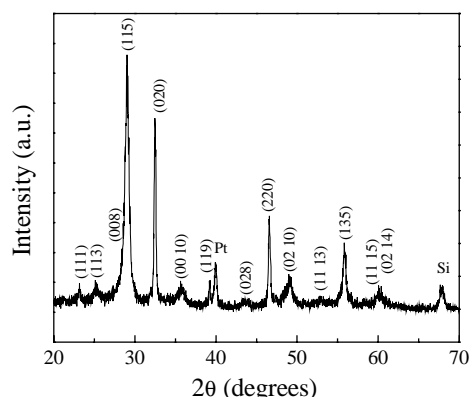


Fig. 1. XRD of SBVN film.

inant polarization along a – b plane. XRD analyses indicated that there is no evidence of secondary phase formation. This demonstrates that with partial substitution of Nb ions by V ions up to 10 at.%, the single-phase layered perovskite was preserved. SEM analysis indicates that the interface between the film and substrate layers are well defined. The SBVN microstructure consisted of well developed plate like grains with considerable volume fractions of micrograins and the grain sizes are in the range of ~ 100 to 300 nm.

The existence of ferroelectric nature in the SBVN thin film was confirmed from the polarization hysteresis, which is displayed in Fig. 2. The ferroelectric hysteresis loop of typical 150 nm SBVN films were measured at an applied field of 666 kV/cm. The SBVN film exhibited a remnant polarization ($2P_r$) of 25 $\mu\text{C/cm}^2$, and the coercive field ($2E_c$) was about 200 kV/cm. The improved polarization in SBVN film is attributed to the increased densification and larger polarizability attained through increased rattling space in the distorted octahedral Nb(V)O₆ of the perovskite block due to the partial substitution of Nb ions (0.69 Å) with smaller V ions (0.58 Å) and also may be related to the suppression of (0 0 1) orientations as evidenced from the XRD of SBVN films. The fatigue endurance was tested with 1 MHz bipolar pulses at 10 V. The SBVN film demonstrated no rapid

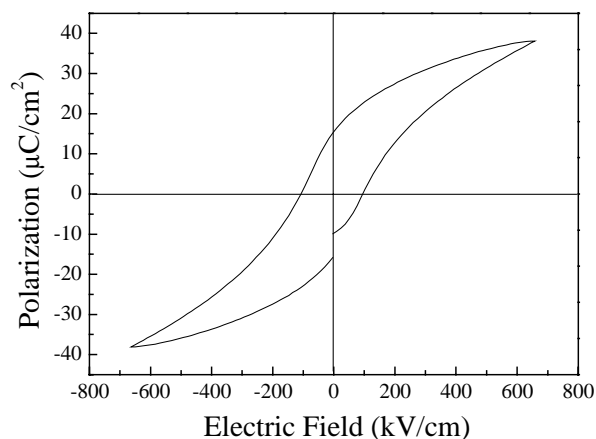


Fig. 2. Hysteresis loop of SBVN film.

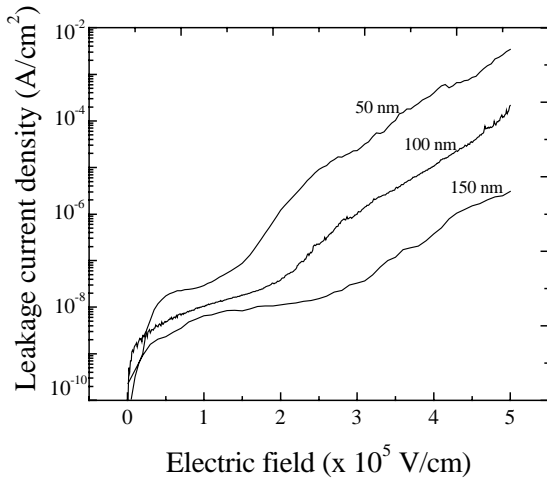


Fig. 3. Leakage current behavior of SBVN film.

fall of remnant polarization and exhibit a minimal fatigue of about 3.2 and $\sim 10\%$ at 10^8 and up to 10^{10} switching cycles, respectively. The fatigue behavior in perovskite thin films are generally explained on the basis of oxygen vacancy and electron/hole injection mechanisms [14]. Oxygen vacancies can be generated during annealing of SBVN films which can be charge compensated by the V ions due to their multiple valence states (V^{4+} and V^{5+}) [7]. Also the improved fatigue behavior may be correlated with the increased lattice distortion of perovskite block of SBVN together with the self-recovery mechanism of $(Bi_2O_2)^{2+}$ layer [1,15].

Fig. 3 shows the I – V characteristics of the SBVN thin film annealed at 700°C for 1 h. The leakage current was improved by increasing the film thickness and the electric field for a steep current increase shift to a lower voltage as the film becomes thinner. The leakage current density decreased from $2.9 \times 10^{-8} \text{ A/cm}^2$ to $6.5 \times 10^{-9} \text{ A/cm}^2$ at 1 V and from $1.2 \times 10^{-6} \text{ A/cm}^2$ to $1.1 \times 10^{-8} \text{ A/cm}^2$ at 2 V with the thickness increasing from 50 to 150 nm.

Further, three different regimes may be distinguished in the I – V characteristic (Fig. 3). At very low electric fields, the current density increases almost linearly with voltage, i.e., the films display nearly Ohmic behavior. This current would be due to the hopping conduction mechanism in a low electric field, because thermal excitation of trapped electrons from one trap site to another dominates transport in the films. At intermediate and higher fields, the current densities are proportional to the square root of the applied electric field because the current density increases much faster on slightly increasing the applied field, which suggests that the leakage current density is limited by a different conduction mechanism from that in the low field region.

Electrical measurements results show that thin SBVN films subjected to an external electric field displayed a linear relationship in the $\log_{10}(J)$ versus $E^{1/2}$ or $\log_{10}(J/E)$ versus $E^{1/2}$ plots (Fig. 4a and b). This dependence is attributed to either the field enhanced Schottky (ES) or the Poole–Frenkel

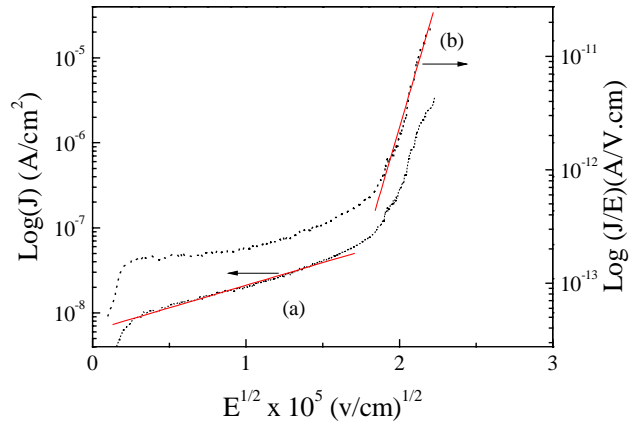


Fig. 4. (a) The $\log_{10}(J)$ vs. $E^{1/2}$ and (b) the $\log_{10}(J/E)$ vs. $E^{1/2}$ plots for SBVN film.

emission (PF) [16,17]. The former is a Schottky emission (ES) process across the interface between a semiconductor (metal) and an insulating film as a result of barrier lowering due to the applied field and the image force. The latter is associated with the field enhanced thermal excitation of charge carriers from traps, sometimes called the internal Schottky effect [17]. These two transport mechanisms are very similar and can be distinguished from the slope measured from the straight line region of the current–voltage (I – V) curve in the form of $\log_{10}(J)$ versus $E^{1/2}$ or $\log_{10}(J/E)$ versus $E^{1/2}$ plots, respectively (Fig. 4a and b). Both ES (Fig. 4a) and PF (Fig. 4b) plots for SBVN films indicate good linearity by least square fit, suggesting that the leakage current mechanism is either ES or PF type.

Fig. 5a shows the plots of $\ln(J/T^2)$ versus $1000/T$ of SBVN films at different voltages. The experimental data fits very well in the form of straight line and the leakage current increased clearly with temperature and applied voltages. The activation energy calculated from the slope varies with the measurement temperature at constant applied voltage indicates the temperature dependence of electrical conductivity of SBVN films. This result demonstrates that the leakage current mechanism of SBVN films is not Fowler–Nordheim (FN) tunneling which is inherently independent of temperature. The slope calculated from the linear region of PF plot (Fig. 4b) is much larger, more than twice than that calculated from ES plot (Fig. 4a). Also the static dielectric constant determined from the capacitance measurements (~ 245 at 10 kHz) are very close to the dielectric constants calculated from slopes of the I – V curve (~ 225). From these results, we conclude that there are three dominant conduction mechanism for the SBVN films, namely Ohmic type at low fields ($< 50 \text{ kV/cm}$), ES limited current flow at intermediate fields (50 – 250 kV/cm) and at higher fields ($> 250 \text{ kV/cm}$) the current is limited by PF mechanism. The slope of Fig. 5a was plotted with the square root of the applied electric field (intermediate region), as shown in Fig. 5b. The barrier height between the film and the Pt electrode was calculated from the intercept and it was estimated to be 1.39 eV. The reported

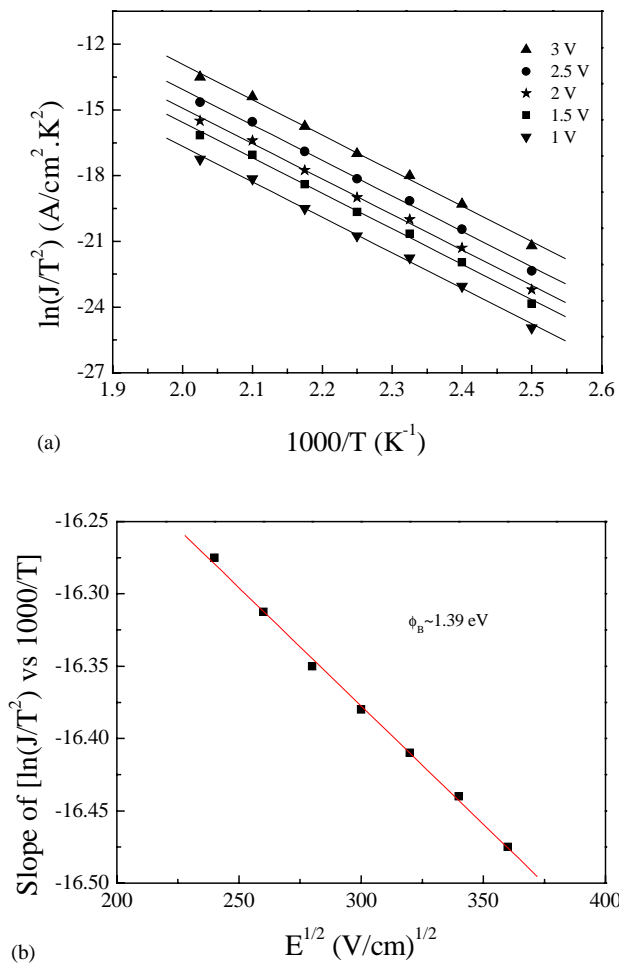


Fig. 5. (a) Variation of $\ln(J/T^2)$ vs. $1000/T$ of the SBVN films at different voltages and (b) variation of slope of (a) with $E^{1/2}$.

Schottky barrier heights for the bismuth layered perovskite thin films are in the range of 0.8–1.37 eV [18]. The estimated barrier height of SBVN films in the intermediate applied field region (50–250 kV/cm) of the I – V curve further confirms the Schottky barrier type conduction.

4. Conclusion

In summary, we successfully investigated the ferroelectric properties and leakage current mechanisms of SBVN films prepared by rf-sputtering. The films showed excellent ferroelectric properties in terms of larger remnant polarization ($2P_r$) of $25 \mu\text{C}/\text{cm}^2$ ($2E_c \sim 200 \text{ kV}/\text{cm}$), fatigue free characteristics up to $\geq 10^8$ switching cycles and lower current density of $10^{-8} \text{ A}/\text{cm}^2$ at $100 \text{ kV}/\text{cm}$. The ferroelectric

properties are comparable to those previously reported for V-doped SBT films. We have unambiguously differentiated experimentally the ES and PF mechanism responsible for electrical transport at different electric field regimes in SBVN films.

References

- [1] C.A. Paz de Araujo, J.D. Cuchlaro, L.D. McMillan, M.C. Scott, J.F. Scott, Fatigue-free ferroelectric capacitors with platinum electrodes, *Nature* (London) 374 (1995) 627.
- [2] O. Auciello, J.F. Scott, R. Ramesh, The physics of ferroelectric memories, *Phys. Today* 51 (1998) 22.
- [3] J. Lettieri, M.A. Zurbuchen, Y. Jia, D.G. Schlom, S.K. Streiffer, M.E. Hawley, Epitaxial growth of non-*c*-oriented $\text{SrBi}_2\text{Nb}_2\text{O}_9$ on (1 1 1) SrTiO_3 , *Appl. Phys. Lett.* 76 (2000) 2937.
- [4] G. Asayama, J. Lettieri, M.A. Zurbuchen, Y. Jia, S. Trolier-McKinstry, D.G. Schlom, S.K. Streiffer, J.-P. Maria, S.D. Bu, C.B. Eom, *Appl. Phys. Lett.* 80 (2002) 2371.
- [5] E.C. Subbarao, A family of ferroelectric bismuth compounds, *Phys. Chem. Solids* 23 (1962) 665.
- [6] S. Ezhilvalavan, J.M. Xue, J. Wang, Dielectric relaxation in $\text{SrBi}_2(\text{V}_{0.1}\text{Nb}_{0.9})_2\text{O}_9$ layered perovskite ceramics, *Mater. Chem. Phys.* 75 (2002) 50.
- [7] S. Ezhilvalavan, J.M. Xue, J. Wang, Evidence of lower valence state of vanadium on the dielectric relaxation of ferroelectric $\text{SrBi}_2(\text{V}_{0.1}\text{Nb}_{0.9})_2\text{O}_9$, *J. Phys. D: Appl. Phys.* 35 (2002) 2254.
- [8] Y. Wu, G. Cao, Enhanced ferroelectric properties and lowered processing temperatures of strontium bismuth niobates with vanadium doping, *Appl. Phys. Lett.* 75 (1999) 2650.
- [9] S.Y. Chen, B.C. Lan, C.S. Taso, Film structure and ferroelectric properties of vanadium-doped $\text{Sr}_{0.8}\text{Bi}_{1.2}\text{Ta}_2\text{O}_9$ thin films, *J. Appl. Phys.* 91 (2002) 10032.
- [10] R. Barz, D.A. Neumayer, P. Majhi, C. Wang, S.K. Dey, Control of bismuth volatility in SBT by vanadium doping, *Integr. Ferroelectrics* 39 (2001) 61.
- [11] R.R. Das, P. Bhattacharya, W. Perez, R.S. Katiyar, Electrical properties of non-*c*-axis oriented $\text{SrBi}_2(\text{Ta}_{0.95}\text{V}_{0.5})_2\text{O}_9$ thin films, *J. Mater. Sci.* 38 (2003) 1171.
- [12] Ch. Schwan, P. Haibach, G. Jakob, J.C. Matinez, H. Adrian, Structural and electrical characterization of $\text{SrBi}_2\text{Nb}_2\text{O}_9$ thin films deposited on $\text{Yb}_2\text{Cu}_3\text{O}_{7-\delta}$ and Nb doped SrTiO_3 , *J. Appl. Phys.* 86 (1999) 960.
- [13] S. Bhattacharya, S.S.N. Bharadwaja, S.B. Krupanidhi, Alternating current conduction behavior of excimer laser ablated $\text{SrBi}_2\text{Nb}_2\text{O}_9$ thin films, *J. Appl. Phys.* 88 (2000) 4294.
- [14] S.B. Desu, D.P. Vijay, Novel fatigue-free layered structure ferroelectric thin films, *Mater. Sci. Eng. B32* (1995) 75.
- [15] B.H. Park, B.S. Kang, S.D. Bu, T.W. Noh, J. Lee, W. Jo, Lanthanum-substituted bismuth titanate for use in non-volatile memories, *Nature* (London) 401 (1999) 682.
- [16] S.M. Sze, *Physics of Semiconductor Devices*, 2nd ed., Wiley, New York, 1981.
- [17] J. O'Dwyer, *Theory of Electrical Conduction and Breakdown in Solid Dielectrics*, Clarendon, Oxford, UK, 1973.
- [18] K. Watanabe, A.J. Hartmann, R.N. Lamb, J.F. Scott, Electronic characteristics of the $\text{SrBi}_2\text{Ta}_2\text{O}_9$ –Pt junction, *J. Appl. Phys.* 84 (1998) 2170.